RESEARCH PAPER

Epigenetics 7:12, 1379–1390; December 2012; © 2012 Landes Bioscience

Sulforaphane causes a major epigenetic repression of *myostatin* in porcine satellite cells

Huitao Fan, Rui Zhang, Dawit Tesfaye, Ernst Tholen, Christian Looft, Michael Hölker, Karl Schellander and Mehmet Ulas Cinar*

Institute of Animal Science; Animal Breeding and Husbandry Group; University of Bonn; Bonn, Germany

Keywords: sulforaphane, satellite cell, myostatin, epigenetic repression, pig

Abbreviations: 5-aza-dC, 5-aza-2'-deoxycytidine; ATF, activating transcription factor; CREB, cAMP response element binding protein; ChIP, chromatin immunoprecipitation; DNMT, DNA methyltransferase; EAAs, essential amino acids; FBS, fetal bovine serum; FST, follistatin; FoxO1, forkhead box O1; GAPDH, glyceraldehyde 3-phosphate dehydrogenase; GDF8, growth differentiation factor 8; GM, growth medium; HDAC, histone deacetylase; HRP, horseradish peroxidase; HPRT1, hypoxanthine phosphoribosyltransferase 1; hSGT, human small glutamin-rich tetratricopeptide repeat-containing protein; MEF2, myocyte enhancer factor 2; MEMα, minimum essential medium α; miRNAs, microRNAs; MSTN, myostatin; MyoD, myoblast determination protein; NPDFs, nasal polyp-derived fibroblasts; PBMC, peripheral blood mononuclear cells; PBS, phosphate-buffered saline; qRT-PCR, quantitative real time PCR; RYR1, ryanodine-receptor gene; SD, standard deviations; SFN, sulforaphane; Smad7, Smad family member 7; Smurf1, Smad specific E3 ubiquitin protein ligase 1; Ct, threshold cycle; TGF-β, transforming growth factor-β; TSA, trichostatin A; UTR, untranslated region

Satellite cells function as skeletal muscle stem cells to support postnatal muscle growth and regeneration following injury or disease. There is great promise for the improvement of muscle performance in livestock and for the therapy of muscle pathologies in humans by the targeting of myostatin (MSTN) in this cell population. Human diet contains many histone deacetylase (HDAC) inhibitors, such as the bioactive component sulforaphane (SFN), whose epigenetic effects on *MSTN* gene in satellite cells are unknown. Therefore, we aimed to investigate the epigenetic influences of SFN on the *MSTN* gene in satellite cells. The present work provides the first evidence, which is distinct from the effects of trichostatin A (TSA), that SFN supplementation in vitro not only acts as a HDAC inhibitor but also as a DNA methyltransferase (DNMT) inhibitor in porcine satellite cells. Compared with TSA and 5-aza-2'-deoxycytidine (5-aza-dC), SFN treatment significantly represses *MSTN* expression, accompanied by strongly attenuated expression of negative feedback inhibitors of the MSTN signaling pathway. miRNAs targeting *MSTN* are not implicated in posttranscriptional regulation of *MSTN*. Nevertheless, a weakly enriched myoblast determination (MyoD) protein associated with diminished histone acetylation in the MyoD binding site located in the *MSTN* promoter region may contribute to the transcriptional repression of *MSTN* by SFN. These findings reveal a new mode of epigenetic repression of *MSTN* by the bioactive compound SFN. This novel pharmacological, biological activity of SFN in satellite cells may thus allow for the development of novel approaches to weaken the MSTN signaling pathway, both for therapies of human skeletal muscle disorders and for livestock production improvement.

Introduction

Pigs is an economically important animal in livestock production, as well as in biomedical studies for humans because of the similarity in physiology, organ development and disease progression.[1] Skeletal muscle growth is one of the major economic traits in meat production. Postnatal muscle maintenance and growth rely on the activation of a unique population of quiescent "satellite cells" (referred to as muscle stem cells), which are capable of self-renewal and myogenic differentiation to form hypernucleated myotubes.[2,3] Satellite cells can be also activated under injury and pathological conditions and contribute to muscle repair and regeneration.[3] Nevertheless, little is known about the effects of bioactive compounds on this multipotent muscle cell population and the mechanisms that mediate their effects.

Sulforaphane (SFN), an isothiocyanate derived from cruciferous vegetables, is a common bioactive compound that has the ability to inhibit type I and II histone deacetylases (HDAC), and is also an antioxidant, anti-carcinogenic and chemotherapeutic agent.[4,5] In this context, we became interested in the HDAC inhibitor property of SFN. In human colorectal cancer cells and prostate epithelial cells, this HDAC inhibition was accompanied by increased histone acetylation in global histone H3, H4 and *P21* gene promoter region, associated with elevated expression of P21 protein.[5,6] In vivo studies with SFN-fed

*Correspondence to: Mehmet Ulas Cinar; Email: ucin@itw.uni-bonn.de
Submitted: 07/16/12; Revised: 10/14/12; Accepted: 10/19/12
http://dx.doi.org/10.4161/epi.22609

©2012 Landes Bioscience. Do not distribute.

mice, HDAC activity was inhibited significantly in various tissues with a concomitant increase in global and local histone acetylation.[7] In healthy human volunteers, oral consumption of SFN-rich broccoli sprouts resulted in strong HDAC inhibition associated with histone hyperacetylation at 3 and 6 h in peripheral blood mononuclear cells (PBMC).[8] However, as a novel natural HDAC inhibitor, the potential epigenetic effects of SFN supplementation on skeletal muscle cells remain undiscovered.

Myostatin (MSTN; previously called growth differentiation factor 8, GDF8) is a member of the transforming growth factor-β (TGF-β) superfamily and a potent inhibitor of skeletal muscle growth.[9] MSTN can also block satellite cell activation and negatively regulate self-renewal of satellite cells.[10] It has been identified that follistatin (FST), Smad family member 7 (Smad7), Smad specific E3 ubiquitin protein ligase 1 (Smurf1) and human small glutamin-rich tetratricopeptide repeat-containing protein (hSGT) are involved in the MSTN pathway and inhibit MSTN activity to attenuate MSTN signaling.[11] In the skeletal muscle field, epigenetic research has emerged only during the last years.[12] Numerous studies have unveiled that epigenetic alterations, including DNA methylation and histone modifications, are important players in finely tuned regulation of gene expression. Small non-coding microRNAs (miRNAs), capable of inducing stable changes in gene expression without altering the sequence of genes, also contribute to the epigenetic landscape.[13] Recently, evidence is accumulating supporting a posttranscriptional regulatory role for miRNAs in the regulation of *MSTN* expression. Data from Drummond et al. show that rapid increase of miR-499 expression by essential amino acids (EAAs) results in the suppression of *MSTN* expression in human skeletal muscle.[14] Allen and Loh have shown that miR-27b targets 3' untranslated region (3'UTR) of *MSTN* efficiently and may contribute to fast-specific and glucocorticoid-dependent *MSTN* expression in skeletal muscle.[15] In a trans-regulatory manner, transcription factor forkhead box O1 (FoxO1) could bind to the mouse *MSTN* promoter and activate its activity to upregulate *MSTN* expression.[16] Transcriptional activity of human *MSTN* promoter was strongly enhanced by myocyte enhancer factor 2 (MEF2) binding to the element present in the promoter region.[17] However, the ability and mechanism of SFN to epigenetically regulate the *MSTN* gene in satellite cells are unknown.

Taking the above observations into account, the objective of this study was to test the hypothesis that SFN supplementation influences satellite cell growth and that epigenetic mechanisms account for *MSTN* gene modulation in response to SFN exposure. In the present study, we also employed the typical epigenetic reagents 5-aza-2'-deoxycytidine (5-aza-dC) and trichostatin A (TSA) and compared their effects to those of SFN treatment. We show that, different from what occurs with TSA, SFN and 5-aza-dC significantly suppress MSTN expression and inhibit HDAC activity as well as *DNA methyltransferase (DNMT)* expression in porcine satellite cells. If its effects are verified and applied to in vivo models, SFN may have therapeutic benefits in the treatment of human skeletal muscle disorders and practical value in meat production.[18]

Results

Epigenetic reagents affect porcine satellite cell growth and inhibit HDAC activity. In this study, we followed cell culture procedure as shown in **Figure 1A**. By design, we selected three serial doses (5 μM, 10 μM and 15 μM) of SFN to avoid oxidative stress and apoptosis, which occurs at higher concentrations in vitro.[19,20] Cells were harvested 48 h after exposure, as it is known that 15 μM SFN inhibits HDAC activity and increases histone acetylation level in prostate cell lines after 48 h treatment.[6] For 5-aza-dC, 10 μM concentration was selected because it is the optimal dose to upregulate both *FST* isoforms (*FST288* and *FST315*).[21] For TSA, we used the general concentration of 50 nM in accordance with previous reports, to serve as a positive control.[22,23] Almost all of the satellite cells were not viable after treatment at day 2 (data not shown); therefore, we selected day 3 (the myoblast stage) to start the treatment. To examine the cytotoxic effects of SFN, TSA and 5-aza-dC treatments on porcine satellite cell growth, we determined cell viability (**Fig. 1B**) and cell proliferation rate (**Fig. 1C**). No difference in cell viability was observed, with the exception of an increase in the SFN5 group. Only the 5-aza-dC and SFN15 groups showed reduction of cell proliferation two days after treatment. Given that 5-aza-dC is a DNMT inhibitor, we first quantified *DNMT1* mRNA expression. In addition to the 5-aza-dC group, *DNMT1* transcripts were also remarkably decreased in the SFN10 and SFN15 groups (**Fig. 1D**). These results indicated that SFN10 was the optimal group for our experiments. To confirm this and the pro-apoptotic effect of SFN, we examined caspase 3 and caspase 9 activity, which are related to apoptosis induced by SFN.[24,25] As shown in **Figure 1E and F**, caspase activities were inhibited, except for caspase 3 in TSA group. Then, we selected the SFN10 group and analyzed HDAC activity in different treatments. In line with previous reports, relative HDAC activities were significantly inhibited in all three treatments (**Fig. 1G**, lower panel). However, global acetylation levels in histone H3 and H4 were notably decreased in 5-aza-dC and SFN10 groups, which differed from the highly elevated histone acetylation observed in the TSA group (**Fig. 1G**, upper panel).

FST variants were not involved in epigenetic effects of SFN on satellite cells. Acting as a potent HDAC inhibitor, TSA can induce the natural MSTN antagonist FST.[23,26] Our initial interest was focused on whether SFN exhibited a similar mechanism as TSA. Therefore, we quantified the total *FST* (**Fig. 2A**) and *FST315* (**Fig. 2B**) expression, as it is not possible to distinguish another porcine *FST* isoform, *FST288,* from *FST315* due to their identical sequence. To gain a full profile of influences of SFN on FST, other two doses (5 μM and 15 μM) were also used. Nevertheless, upregulated total *FST* and *FST315* were not observed in SFN groups. Considering the *DNMT1* alterations, we plotted 31 CpG sites in the second predicted CpG island (**Fig. 2C**) of the porcine *FST* 5' regulatory region and determined their DNA methylation status (**Fig. 2D**). Bisulfite sequencing analysis revealed that all of the 31 CpG sites were sparsely methylated, except for some sporadic methylation sites. Taken

©2012 Landes Bioscience. Do not distribute.

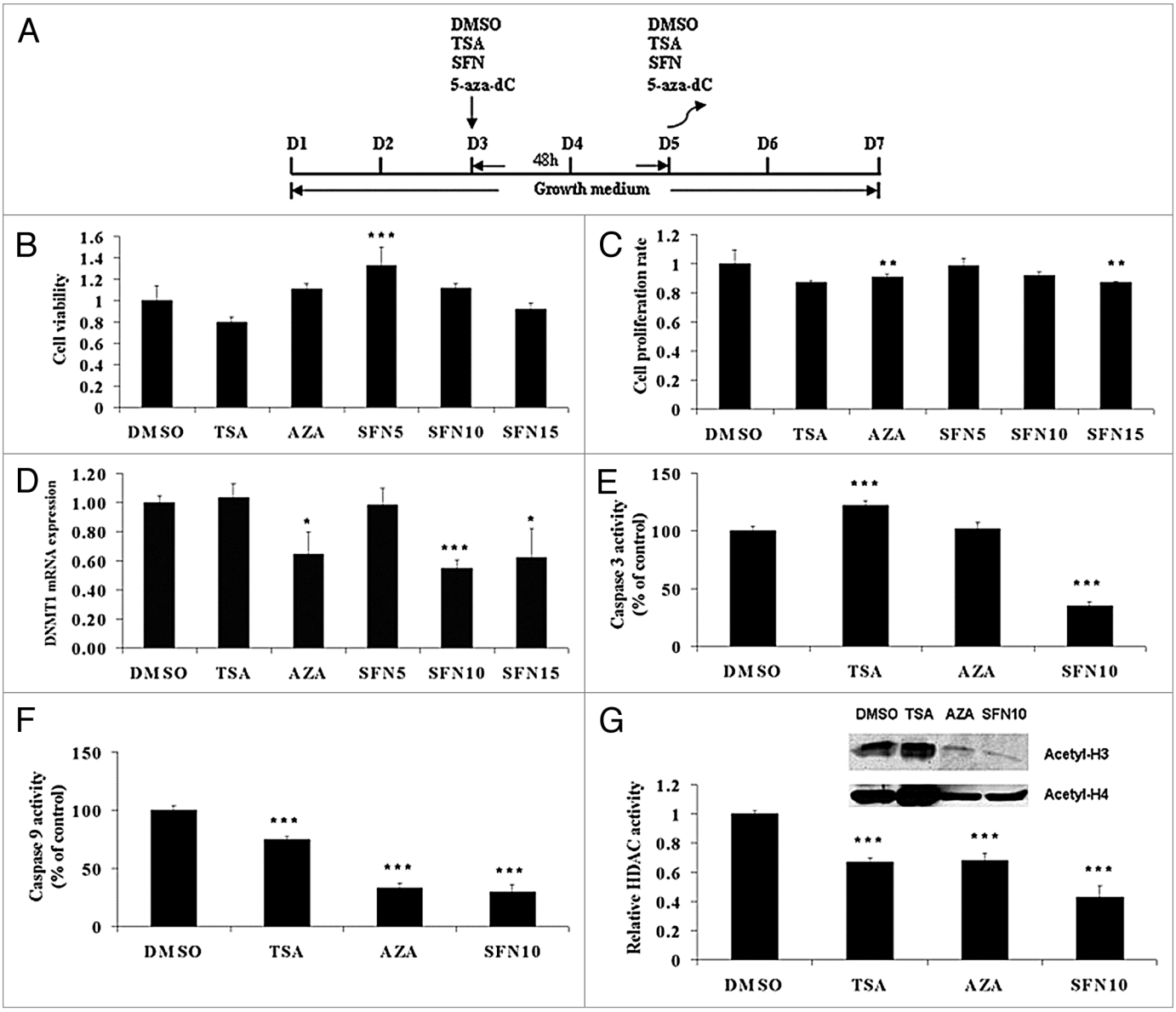


Figure 1. Epigenetic reagents affect porcine satellite cell culture and inhibit HDAC activity. (**A**) Scheme of porcine satellite cell culture and treatment procedure. (**B**) Cells were treated following the procedure as shown in (**A**). Cell viability was determined by WST-1 kit. (**C**) After removal of epigenetic chemicals, cells were allowed to proliferate for 2 d. Then cell proliferation rate was assessed by WST-1 kit. (**D**) *DNMT1* relative mRNA expression was quantified by qRT-PCR after treatments. (**E and F**) Caspase-3 and 9 activity in cultures were evaluated using the caspase-3/CPP32 Colorimetric Assay Kit and caspase-9 Colorimetric Assay Kit, respectively. (**G**) Relative HDAC activity (lower panel) was examined using the Color-de-Lys HDAC colorimetric activity assay kit. Equal amounts of isolated histone protein were subjected to western blotting analysis to investigate acetylated histone H3 and H4 levels (upper panel). The results represent the mean ± standard deviations (SD) of three independent experiments each performed in duplicate (*p < 0.05; **p < 0.01; ***p < 0.001).

©2012 Landes Bioscience. Do not distribute.

together, these results indicate that *FST* is not induced by SFN and not involved in SFN effects on porcine satellite cells.

MSTN and its signaling pathway were inhibited by SFN treatment. MSTN is a potent negative regulator of myogenesis, and inactivation of MSTN results in heavy muscle growth.[27] Given that *FST* gene expression was not induced by SFN, we then studied *MSTN* as the candidate gene and determined its expression levels, which were significantly upregulated by TSA and downregulated by 5-aza-dC and SFN (**Fig. 3A**). In this experiment, other two doses of SFN (5 μM and 15 μM) were also tested to gain a full profile of influences of SFN on MSTN signaling pathway genes. Besides FST, Smad7, Smurf1 and hSGT have also been identified as inhibitors of the MSTN signaling pathway in skeletal muscle.[11] Our results show that *hSGT* expression was upregulated in TSA, 5-aza-dC and SFN15 groups (**Fig. 3B**). In comparison, *Smad* (**Fig. 3C**) and *Smurf1* (**Fig. 3D**) were only upregulated in SFN treatment groups. Collectively, our observations thus suggested that MSTN itself and its pathway were more strongly attenuated by SFN.

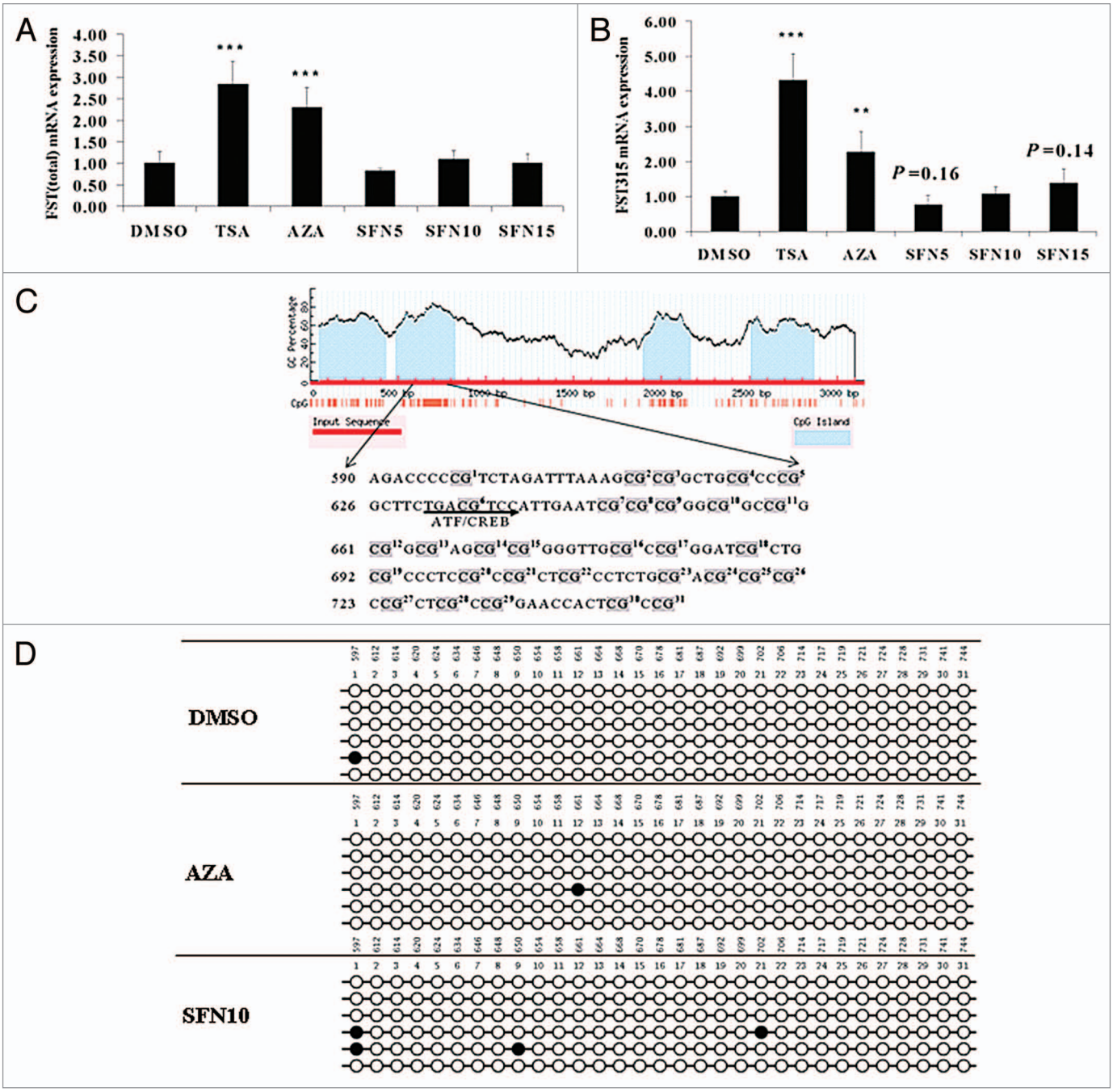


Figure 2. *FST* variants were not involved in epigenetic effects of SFN on satellite cell. (**A and B**) Total *FST* and *FST315* mRNA levels were quantified by qRT-PCR after treatments. The results represent the mean ± standard deviations (SD) of three independent experiments each performed in duplicate (**p < 0.01; ***p < 0.001). (**C**) CpG islands in the *FST* promoter region were predicted by MethPrimer online (upper panel). Thirty-one numbered CpG dinucleotides were mapped in genomic sequence (lower panel). (**D**) DNA methylation status within CpG island 2 spanning putative activating transcription factor (ATF)/cAMP response element binding protein (CREB) binding site was quantified by bisulfite sequencing PCR. A minimum of six positive clones were randomly picked for sequencing with M13 primers. Sequencing results were visualized by QUMA software. Unfilled (white) circles correspond to unmethylated Cs and filled (black) circles correspond to methylated Cs.

Predicted miRNAs targeting porcine MSTN 3' UTR region were not involved in epigenetic repression of MSTN. miRNAs can silence mRNAs by endonuclease cleavage, translational repression and mRNA degradation.[28] In order to investigate whether specific miRNAs play regulatory roles in modulating *MSTN* transcription, we identified several miRNA targeting *MSTN*, including miR-21, miR-26a, miR-29abc and miR-181a, and also obtained experimentally confirmed miRNAs such as miR-27ab,[15] miR-208b,[29] miR-499[30] previously shown to target *MSTN*. miR-208b and miR-499 expression was not able to be determined, as indicated by threshold cycle (Ct) value above 35 cycles (data not shown). All of the miRNAs, except miR-27b, were

©2012 Landes Bioscience. Do not distribute.

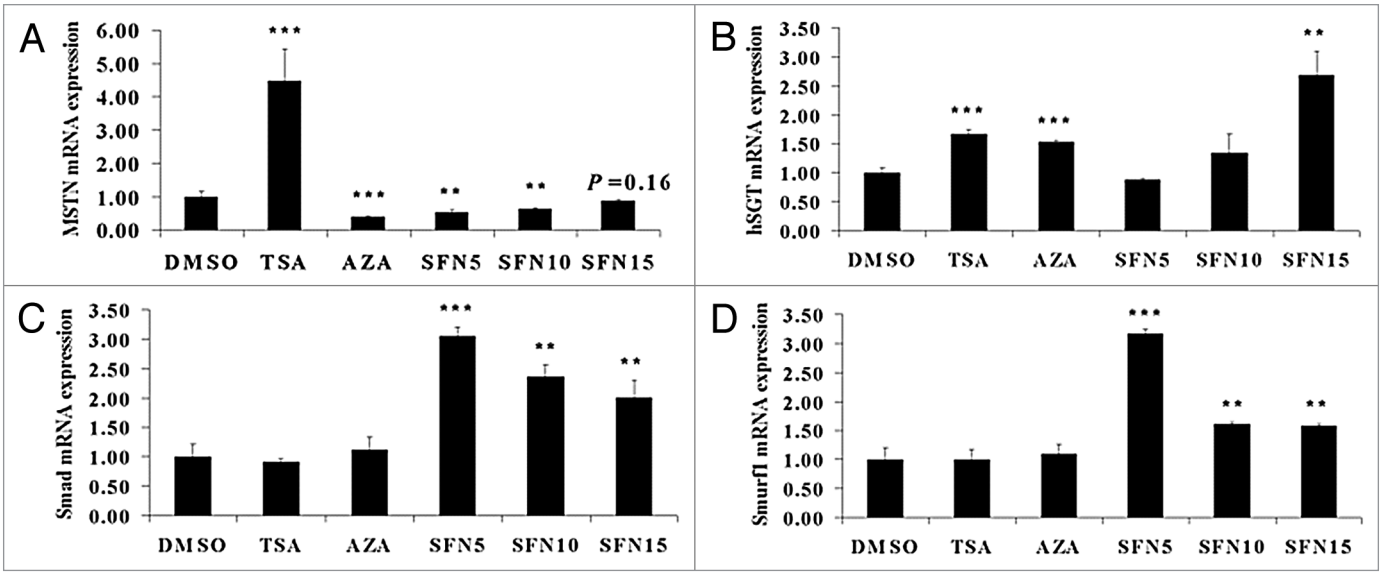


Figure 3. MSTN and its signaling pathway were inhibited by SFN treatment. qRT-PCR was performed to quantify *MSTN* (**A**), *hSGT* (**B**), *Smad7* (**C**) and *Smurf1* (**D**) mRNA level. The results represent the mean ± standard deviations (SD) of three independent experiments each performed in duplicate (**p < 0.01; ***p < 0.001).

remarkably downregulated in the 5-aza-dC group (**Fig. 4A–H**). miR-29a and miR-29b expression dramatically decreased in the SFN group (**Fig. 4E and F**). Only miR-29b exhibited notably increased expression in the TSA group (**Fig. 4F**).

Myoblast determination protein (MyoD) can bind to *MSTN* promoter to regulate its transcription involving histone deacetylation by SFN. Accumulating evidences report that *MSTN* expression could be regulated at the transcriptional level. Further analysis of porcine *MSTN* promoter sequence revealed three putative MyoD binding sites (**Fig. 5A**). To study the transcriptional regulation of the *MSTN* gene, we next examined whether MyoD would be recruited to the promoter regions of *MSTN*. ChIP with an antibody against MyoD confirmed that endogenous MyoD was present in binding site 1 of *MSTN* promoter region, indicating that MyoD interacts with *MSTN* to regulate *MSTN* transcription (**Fig. 5B**). In order to examine MyoD availability as transcription factor, we quantified MyoD mRNA and protein level. In accordance with mRNA expression, MyoD protein level was significantly elevated in the TSA group but decreased in 5-aza-dC and SFN10 groups (**Fig. 5C**). To examine the recruitment of MyoD to the *MSTN* promoter region, ChIP was conducted to quantify the relative enrichment. ChIP results demonstrated weak recruitment of MyoD in 5-aza-dC and SFN10 group, compared with a robust recruitment of MyoD in the TSA group (**Fig. 5D**). We were unable to investigate the epigenetic regulatory role of DNA methylation in *MSTN* gene transcription because no CpG island in the promoter region of porcine *MSTN* is available. Moreover, ChIP assays were performed to determine the local histone acetylation status of MyoD response element. In contrast to the dramatic histone hyperacetylation in TSA group, hypoacetylation status of histone H3 and H4 was observed in the 5-aza-dC and SFN10 groups (**Fig. 6A and B**). Taken together, these results suggest diminished MyoD and promoter-specific hypoacetylation could downregulate *MSTN* expression at transcription level.

Discussion

For understanding human diseases, pig represents a promising model for biomedical research because it closely resembles and reflects human biology.[31] In this study, we provided the first evidence for both SFN and 5-aza-dC as inhibitor of HDAC and *DNMT* in porcine satellite cells, demonstrating epigenetic mechanisms that are different from the ones exerted by TSA. A previous report has described protective effects of SFN treatment on rat skeletal muscle damage and oxidative stress,[32] but not in the context of HDAC inhibition. To our knowledge, this is the first study of the effect of SFN in satellite cells. As for 5-aza-dC, there is only one report demonstrating that human skeletal muscle *ryanodine-receptor gene* (*RYR1*) transcription was reactivated after treatment with 5-aza-dC,[33] but without evidence for epigenetic effects of 5-aza-dC on myoblasts.

In this study, we investigated the potential epigenetic effects of SFN, TSA and 5-aza-dC treatments on porcine satellite cell growth. Our results demonstrate that none of SFN, 5-aza-dC and TSA influenced the cell viability, except for 5 μM SFN. The increased cell viability in the SFN5 group may indicate the protective effects of SFN on satellite cells at lower concentration.[32] We also found that cells in 5-aza-dC and SFN15 groups had a reduction in cell proliferation as compared with negative control. SFN at 10 μM did not have anti-proliferative effect in satellite cells. The reduction detected after 2 d of treatment may be due to apoptotic response to 5-aza-dC and high dose of SFN.[6,24,25] We then aimed to investigate the effects of 5-aza-dC on the DNA methylation status, and how the alteration of promoter region methylation affected gene expression. *DNMT1*

©2012 Landes Bioscience. Do not distribute.

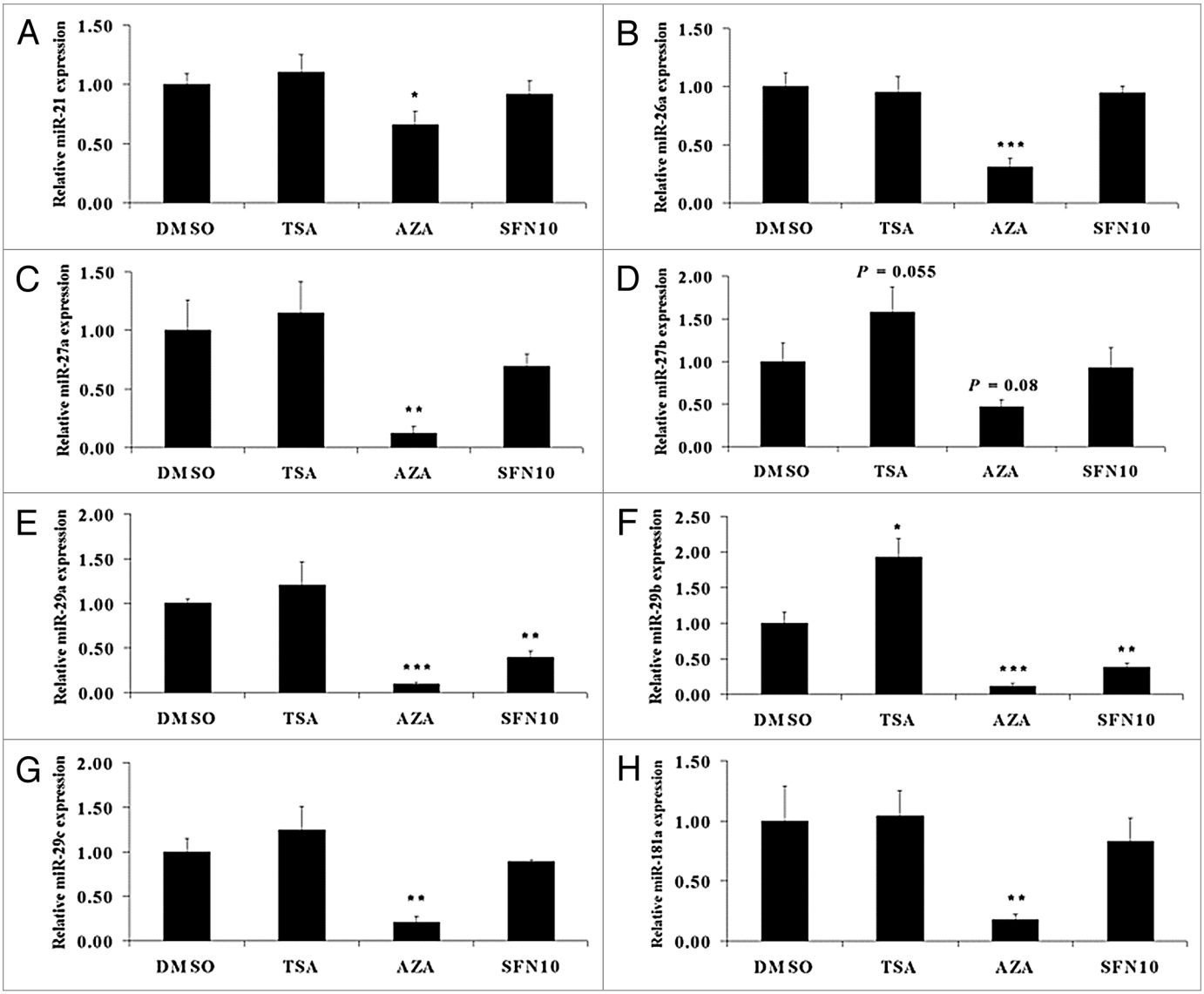


Figure 4. Predicted miRNAs targeting porcine *MSTN* 3'UTR region were not implicated in *MSTN* epigenetic repression. qRT-PCR was undertaken to quantify miR-21 (**A**), miR-26a (**B**), miR-27a (**C**), miR-27b (**D**), miR-29a (**E**), miR-29b (**F**), miR-29c (**G**) and miR-181a (**H**) expression level. The results represent the mean ± standard deviations (SD) of three independent experiments each performed in duplicate (*p < 0.05; **p < 0.01; ***p < 0.001).

expression was significantly suppressed in the 5-aza-dC group, and also in HDAC inhibitor group (SFN10 and SFN15). These results are in line with previous studies that report that SFN significantly decreased the expression of *DNMT1* in response to SFN in breast cancer cells[34] and prostate cancer cells.[35] Gomyo et al.[24] and Singh et al.[25] reported that 5-aza-dC and SFN-induced apoptosis is associated with activation of caspase-3 and caspase-9. SFN dramatically reduced the activity of caspase-3 in the cortex and hippocampus after hypoxia-ischemia insult[36] and was able to counteract rat skeletal muscle damage induced by acute exercise.[32] In our study, we determined caspase-3 and caspase-9 activities, which decreased in 5-aza-dC and SFN10 groups, suggesting that 10 μM SFN had no pro-apoptotic effect in the cells. Multiple studies from cell to human have established that SFN is an effective inhibitor of HDAC activity, with evidence for increased global and local histone acetylation status.[37] However, our work shows that SFN and 5-aza-dC are potent inhibitors of HDAC activity, but decreased global acetylated histones H3 and H4, which differ from the effect observed with TSA. Although HDAC inhibitor is expected to induce hyperacetylation, no changes in the H3 or H4 acetylation,[20] and even histone deacetylation,[38] were observed. Following similar treatment conditions as ours (48 h exposure to 15 μM SFN), Pledgie-Tracy et al. demonstrated significantly inhibited HDAC activity in four human breast cancer cell lines without significant changes in the acetylation of H3 or H4.[20] Another two HDAC inhibitors, MS-275 or SK-7068, also effectively inhibited cellular HDAC activity in human gastric adenocarcinoma cells (SNU-16) and caused decreased H3 or H4 acetylation after 48 h, 72 h and 96 h exposure.[38] These findings indicate that HDAC inhibitory effects by

©2012 Landes Bioscience. Do not distribute.

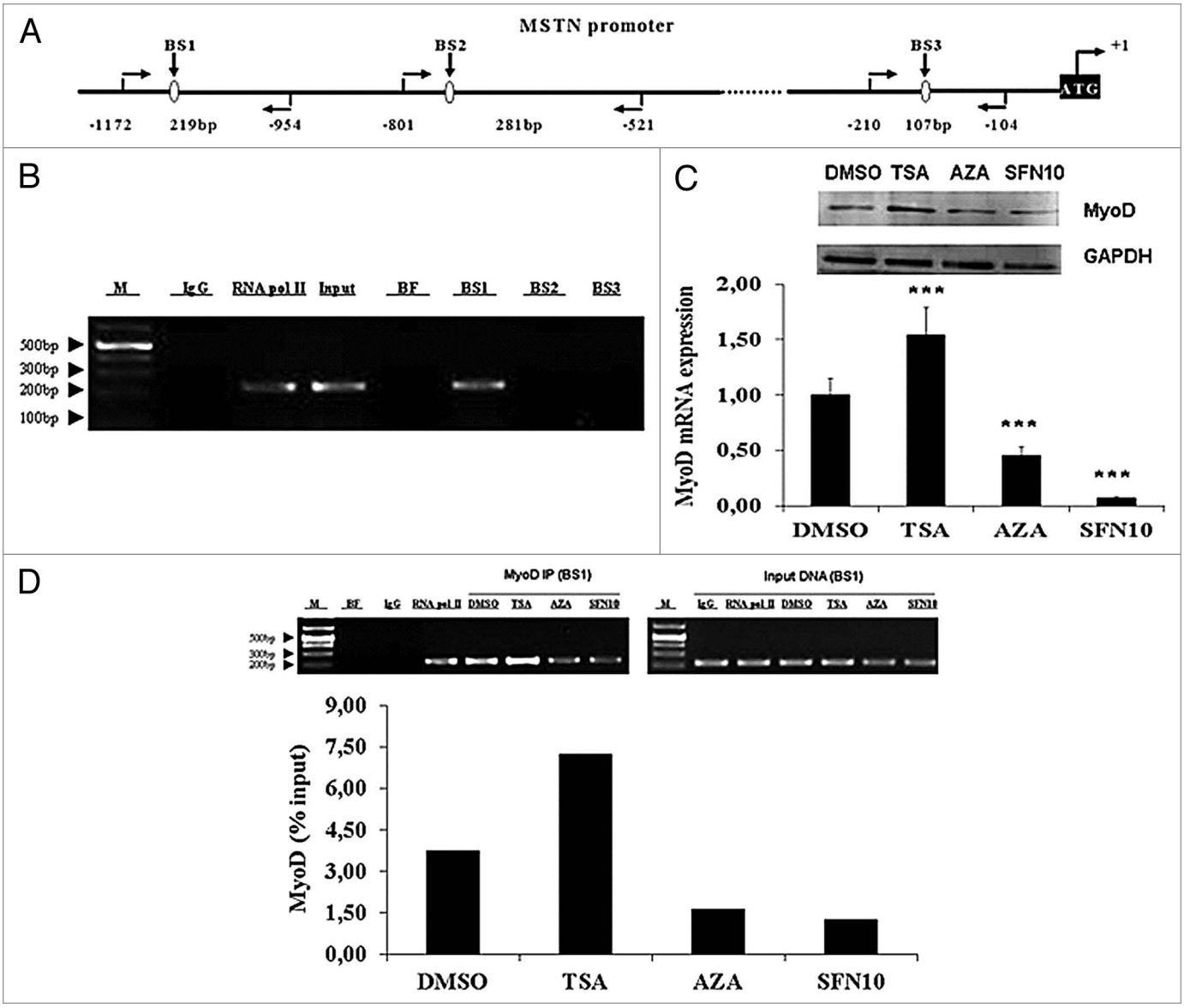


Figure 5. MyoD expression and occupancy in the *MSTN* promoter were significantly diminished by SFN and 5-aza-dC. (**A**) Schematic representation of three potential MyoD binding sites and PCR-amplified fragments located in *MSTN* promoter region. (**B**) ChIP was performed for MyoD recruitment to *MSTN* promoter following 48 h treatment. Soluble chromatin was immunoprecipitated with antibodies against rabbit IgG, RNAP II and MyoD. Immunoprecipitates were subjected to PCR with primer-pairs for each amplicon indicated in (**A**). The sequences of primer pairs are described in **Table 1**. As a negative control, a set of primers were used to amplify binding free region that was not expected to interact with the MyoD. Amplification products were resolved in 2% agarose gel stained with ethidium bromide. M, DNA marker; BF, MyoD binding free region; BS1-3, MyoD binding site 1–3. (**C**) MyoD mRNA (lower part) and protein (upper part) expression were quantified by qRT-PCR and western blotting, respectively. The results represent the mean ± standard deviations (SD) of three independent experiments each performed in duplicate (***$p < 0.001$). (**D**) Abundance of MyoD binding in BS1 of *MSTN* promoter region was determined by quantitative PCR following ChIP assay with MyoD antibody (lower part). Data are shown as a ratio to the input DNA. The PCR products were generated and visualized in 2% agarose gel (upper part). M, DNA marker; BF, MyoD binding free region; BS1, MyoD binding site 1.

SFN withdraw, and cannot last longer to maintain histone acetylation in porcine satellite cells.

FST is one of the regulatory proteins which is capable of binding directly to MSTN, inhibiting its activity and acting as a potent MSTN antagonist.[39] Both *FST315* and total *FST* expression increased remarkably in TSA and 5-aza-dC groups, whereas SFN was not able to induce *FST*. Bisulfite sequencing PCR results demonstrated a few sporadic methylated sites. In contrast, a significant increase in *FST* mRNA expression and peptide secretion was detected after 5-aza-dC treatment in human NCI-H295R adrenocortical cells, as well as hypomethylation in *FST* promoter region.[21] The present study suggests that *FST* isoforms were not induced by SFN and that DNA methylation may not be involved in the regulation of *FST* expression.

MSTN inhibits myoblast proliferation and differentiation via a typical TGF-β pathway.[11] Here we show, for the first time, that

©2012 Landes Bioscience. Do not distribute.

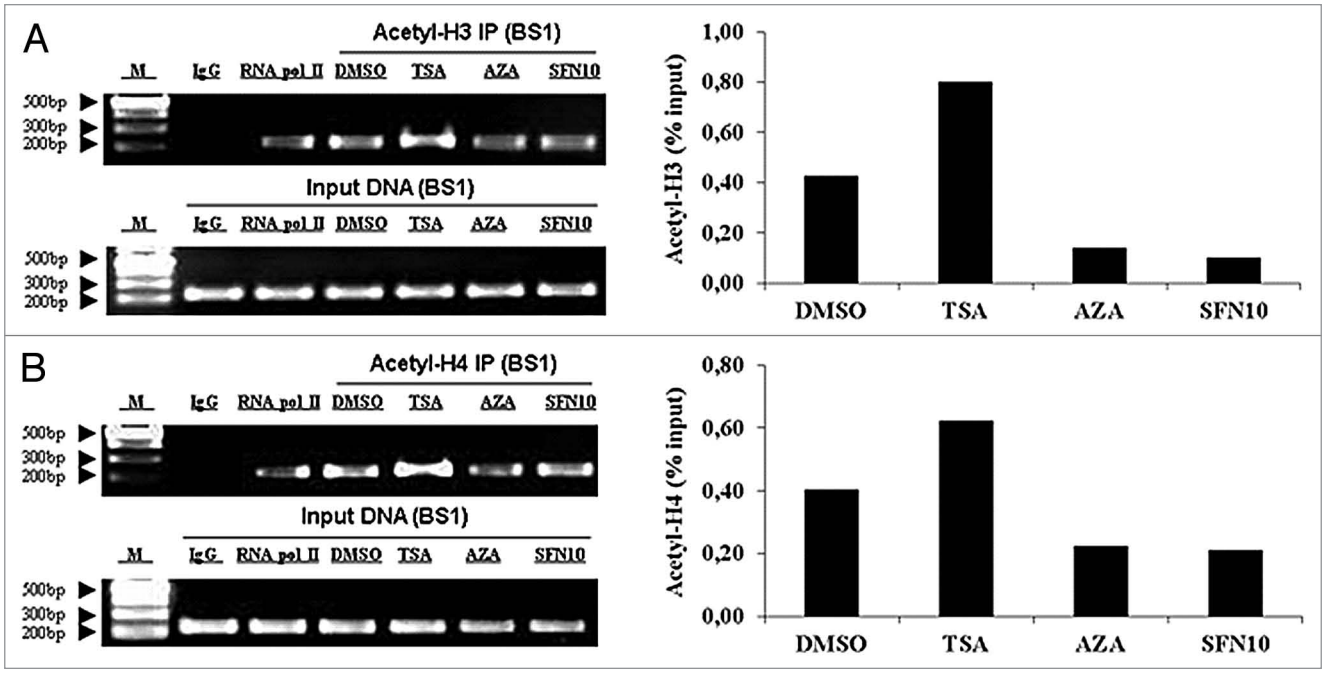


Figure 6. SFN and 5-aza-dC caused weak enrichment of acetylated histones around the *MSTN* BS1. (**A**) Acetyl-histone 3 was examined by quantitative PCR following ChIP assay with MyoD antibody (right part). Amplification products were visualized in a 2% agarose gel (left part). (**B**) Acetyl-histone 4 was determined by quantitative PCR following ChIP assay with MyoD antibody (right part). PCR products were visualized in a 2% agarose gel (left part). Data are normalized to the amount of input chromatin. M, DNA marker; BS1, MyoD binding site 1.

SFN and 5-aza-dC treatments clearly result in attenuated *MSTN* expression. In keeping with previous report that show that TSA increased *MSTN* mRNA expression up to 40-fold in C2C12 myoblast after treatment for 24 h,[40] a substantial increase in *MSTN* expression was observed in the TSA group. These results indicate that these epigenetic reagents affect *MSTN* expression through distinct regulatory mechanisms. In skeletal muscle, several proteins involved in the MSTN signaling pathway have been identified as inhibitors of its secretion, activation, or receptor binding, including FST, Smad7, Smurf1 and hSGT.[11] We determined mRNA expression of these negative regulators in different treatments, which illustrates differential mechanisms involved in the inhibition of the MSTN signaling pathway. Upregulated *FST* and *hSGT* may mainly cause MSTN pathway inhibition in TSA and 5-aza-dC group. Moreover, enhanced *Smad* and *Smurf1* could participate in such inhibition in the SFN group. A recent study has shown that TSA induced expression of *Smad7* in nasal polyp-derived fibroblasts (NPDFs) exposed to TSA (50–400 nM) with TGF-β1 for 24 h.[41] Our results show that TSA did not affect expression of *Smad7*, which may be due to the different treatment and cells. No data are available for SFN or 5-aza-dC regulating *Smad7* expression. As for *Smurf1*, in contrast to no alterations observed in TSA and 5-aza-dC groups, we report for the first time that SFN could upregulate its expression. With regard to *hSGT*, elevated expressions were also observed in TSA, 5-aza-dC and SFN15 groups.

Recently, decreased expression of miR-136 and miR-500 have been detected in low protein fed pigs at finishing stage, which is related to higher *MSTN* mRNA expression.[42] Here, we demonstrate in porcine satellite cells that miRNAs and *MSTN* were not expressed in a reciprocal manner, suggesting that miRNAs may be not involved in the posttranscriptional regulation of *MSTN* expression. We speculate that increased miRNAs expression in TSA group and decreased miRNAs expression in the 5-aza-dC and SFN10 groups are highly linked with deregulated permissive mark histone acetylation, as indicated by global acetylated histone H3 and H4 level (**Fig. 1G**). Upregulation of miR-127 has been observed in T24 human bladder cancer cells treated by 5-aza-dC and another HDAC inhibitor, 4-phenylbutyric acid. Importantly, acetylated histone H3 restored miR-127 expression, confirming that histone acetylation epigenetically regulates miRNA gene expression.[43] Reduced expression of miR-200 family and miR-205 in bladder cancer cells is also caused by repressive histone marks in their promoter region.[44] miRNA microarray analysis revealed 22 downregulated miRNA species and 5 upregulated miRNAs in the breast cancer cell line SKBr3 in response to HDAC inhibitor LAQ824.[45]

Our ChIP assay results confirmed that MyoD was recruited to the first putative binding site in vivo. We also demonstrated by quantitative PCR that MyoD was relatively lowly enriched in 5-aza-dC and SFN10 groups, which coincides with the lower levels of MyoD mRNA and protein abundance. It can be suggested that MyoD could be regulating *MSTN* gene expression by binding to its response element in the promoter region. Spiller et al.[46] reported that one of bovine *MSTN* gene upstream regulatory elements appears to be critical for *MSTN* promoter activity and that MyoD interacts with this binding motif in vitro as well as in vivo to regulate *MSTN* gene expression. More recently, Liu et al.[42]

©2012 Landes Bioscience. Do not distribute.

have described that increased histone H3 acetylation, an activation mark, may account for transcriptional activation of *MSTN* in response to maternal dietary protein at finishing stage in pigs. In our study, compared with hyperacetylation of histone H3 and H4 in the TSA group, hypoacetylation at the MyoD binding site in the 5-aza-dC and SFN10 groups diminishes binding of MyoD to its binding element, inactivating *MSTN* transcription.

In summary, this is the first demonstration that SFN can regulate MSTN and inhibitors of MSTN signaling pathway in porcine satellite cells. Our data revealed the following: (1) both 5-aza-dC and SFN significantly inhibit HDAC activity and *DNMT1* expression. (2) 5-aza-dC, SFN and TSA function by different mechanisms to inhibit *MSTN* expression and negative regulators of the MSTN pathway. (3) Deregulated miRNA may be not involved in epigenetic repression of *MSTN*. (4) Epigenetic repression of *MSTN* by 5-aza-dC and SFN is associated with reduced *MyoD* expression, diminished binding of MyoD to the *MSTN* promoter and hypoacetylation of the MyoD binding site. These results provide new insight into the manipulation of muscle cell phenotypes. In the future, it will be interesting to verify the functional roles of SFN in vivo and evaluate the potentials for its use in the therapy of human muscle diseases and livestock muscle growth.

Materials and Methods

Porcine satellite cells isolation. The right and left semimembranosus muscles from 6 purebred Pietrain piglets at 20 d of age were collected for porcine satellite cells isolation. Piglets were slaughtered by intracardiac injection of T61 (Intervet). All the pigs were kept and slaughtered according to German performance test directions.[47] The porcine satellite cells isolation procedure was outlined by Mau et al.[48] Briefly, the muscle samples were quickly removed, sterilized with 70% ethanol, rinsed in cold phosphate-buffered saline (PBS), minced, and digested with 0.25% trypsin (27250-018, Invitrogen) for 1 h at 37°C with continuous shaking. Digestion was stopped by 20% fetal bovine serum (FBS, 10270106, Invitrogen). The resulting cell suspension was then filtered through 2 × 70 μm (352350, BD Falcon) and 1 × 40 μm cell strainer (352340, BD Falcon). Satellite cells were enriched by using a Percoll (P1644, Sigma-Aldrich) gradient (90%, 40% and 25%) centrifugation. Then the enriched satellite cells were collected and diluted with minimum essential medium α (MEMα, M0894, Sigma-Aldrich) supplemented with 4 mM glutamine (25030, Invitrogen), 100 IU/ml penicillin, 100 μg/ml streptomycin (15140, Invitrogen), 2.5 μg/ml fungizone (15290, Invitrogen) and 10% FBS. After counting by a hemocytometer, aliquots of the cells were frozen in liquid nitrogen until making a pool. Before starting experiments, a uniform pool was made from all aliquots obtained from several isolation procedures.

Cell culture, cell viability and cell proliferation rate. Aliquots of uniform porcine satellite cells pool were thawed and reseeded in gelatin-coated (0.1%, G1890, Sigma-Aldrich) CytoOne cell culture dishes or flasks (USA Scientific, Inc.). All incubations were performed at 37°C under a humidified atmosphere of 5% CO_2 in air. The medium was changed every other day and all experiments were repeated for three times with duplicates. Details of cell culture procedure are shown in **Figure 1A**. At day 3, the cells were exposed to DMSO (7029.1, Carl Roth GmbH), TSA (T8552, Sigma-Aldrich), 5-aza-dC (A3656, Sigma-Aldrich), and SFN (S8044, LKT) for 48h in MEMα with 10% FBS (growth medium, GM). Treatments were categorized into 0.04% DMSO (vehicle control, equal 0.04% DMSO present in other reconstituted chemicals), TSA (50 nM TSA), AZA (10 μM 5-aza-dC), SFN5 (5 μM SFN), SFN10 (10 μM SFN) and SFN15 (15 μM SFN) groups.

WST-1 kit (10008883, Cayman Chemical) was used to quantify cell viability and cell proliferation rate according to the manufacturer's instruction. Cell viability was measured after treatment. Cell proliferation rate was determined after two additional days in GM without treatment.

Measurement of cell apoptosis. Cells were reseeded in gelatin coated plates, followed by a 48 h treatment. Caspase-3 and 9 activity in cultures were measured using the caspase-3/CPP32 Colorimetric Assay Kit (K106-25, Biovision) and caspase-9 Colorimetric Assay Kit (K119-25, Biovision), according to the manufacturer's instructions. Samples were read at 405 nm in a microtiter plate reader (Molecular Devices).

In vitro HDAC activity assay and histone isolation. After treatment at day 5, in vitro HDAC activity was determined using the Color-de-Lys HDAC colorimetric activity assay kit (BML-AK501-0001, Enzo Life Sciences), following the protocol described by the manufacturer. Briefly, approximately 10 μg nuclear extract for each sample was incubated with the HDAC assay buffer and the HDAC colorimetric substrate for 30 min at 37°C. Lysine developer was then added, and the samples were incubated at 37°C for another 30 min. Samples were read at 405 nm using a microtiter plate reader.

Satellite cells were cultured without or with different treatment for 48 h. Histone proteins were then isolated by EpiQuik Total Histone Extraction Kit (OP-0006, Epigentek) according to the manufacturer's manual, followed by western blotting analysis of acetylated histone 3 and histone 4.

Prediction of miRNAs targeting MSTN. To determine the differentially expressed miRNAs targeting *MSTN*, we used two miRNA target prediction algorithms: MicroCosm Targets Version 5 (www.ebi.ac.uk/enright-srv/microcosm/htdocs/targets/v5), and TargetScan.[49] The putative binding sites were further verified by RNAHybrid (http://bibiserv.techfak.uni-bielefeld.de/rnahybrid/submission.html) and RNA22 (http://cbcsrv.watson.ibm.com/rna22.html).

qRT-PCR of miRNA and mRNA. Total RNAs including miRNAs were isolated using miRNeasy Mini Kit (217004, Qiagen) and reverse transcribed using miScript II RT Kit (218161, Qiagen). Total RNAs for mRNA expression were isolated and reverse transcribed as described previously.[4] Primers were designed using the online Primer3 program.[50] Quantitative real time PCR (qRT-PCR) was performed with a StepOnePlus Real-Time PCR System (Applied Biosystems) using miScript SYBR Green PCR Kit (218073, Qiagen) and iTaq SYBR Green Supermix with ROX (172-5850, Bio-Rad) for the detection of miRNAs and mRNAs, respectively. Primers used for the

©2012 Landes Bioscience. Do not distribute.

Table 1. List of primer sequences used in this study

Applications and targets		Primers sequence (5'–3')	GenBank ID
qRT-PCR for mRNA expression	DNMT1	F: GCG GGA CCT ACC AAA CAT R: TTC CAC GCA GGA GCA GAC	DQ060156
	Myostatin	F: GAT TAT CAC GCT ACG ACG GA R: CCT GGG TTC ATG TCA AGT TTC	AY448008
	FST315	F: AGT GAC AAT GCC ACC TAC GC R: CCT CGG TGT CTT CTG AAA TGG	M19529.1
	FSTtotal	F: AAA ACC TAC CGC AAC GAA TG R: CAG AAA ACA TCC CGA CAG GT	NM_001003662
	MyoD	F: TGC AAA CGC AAG ACC ACT AA R: GCT GAT TCG GGT TGC TAG AC	GU249575
	Smurf1	F: CAG CGT CTG GAT CTA TGC AA R: CTA ACA GGC CTC TGC AGT CC	XM_003354460
	Smad7	F: CCA ACT GCA GAC TGT CCA GA R: CAG GCT CCA GAA GAA GTT GG	HM803236
	hSGT	F: GAC CCC GAC AAT GAG ACC TA R: TGA TGC CAT GCT CAT AAA GC	NM_001244392
	HPRT1	F: AAC CTT GCT TTC CTT GGT CA R: TCA AGG GCA TAG CCT ACC AC	NM_001032376.2
qRT-PCR for miRNA expression	ssc-miR-21	F: GCA CCT AGC TTA TCA GAC	
	ssc-miR-26a	F: TTC AAG TAA TCC AGG ATA GGC T	
	ssc-miR-27a	F: TTC ACA GTG GCT AAG TTC TGC	
	ssc-miR-27b	F: TTC ACA GTG GCT AAG TTC TGC	
	ssc-miR-29a	F: CTA GCA CCA TCT GAA ATC GGT TA	
	ssc-miR-29b	F: TAG CAC CAT TTG AAA TCA GT	
	ssc-miR-29c	F: TAG CAC CAT TTG AAA TCG GTT A	
	ssc-miR-181a	F: AAC ATT CAA CGC TGT CGG TGA GTT	
	18S	F: ACG GAC AGG ATT GAC AGA TT	
Bisulfite sequencing PCR	FST-met-nest1	F: TAT TGG GAG ATY GTT TAT YGT AAA T R: CTT AAA ACR AAC CAT TCT	M19529
	FST-met-nest2	F: AGA TTT TYG TTT AGA TTT AAA G R: CAR CAA ATA ATT CCA RCA AA	M19529
ChIP assay	MyoD-BSF	F: TGA ATC AGC TCA CCC TTG ACT R: ATG ATT GGC TCT TGC TCC AC	AY527152
	MyoD-BS1	F: CCA GAC CTT ACC CCA AAT CC R: GCA GTT TGC CTC AGA TTT CC	AY527152
	MyoD-BS2	F: CAG TTG AAA ACT GAG CAC GA R: TTT AGA CAA ACA TTT GAG GAA AAA	AY527152
	MyoD-BS3	F: GTG GAG CAA GAG CCA ATC AT R: ACA ACT TGC CAC ACC AGT GA	AY527152

detection of miRNA and mRNA are listed in **Table 1**. qRT-PCR data were analyzed using the $2^{-\Delta\Delta Ct}$ method[51] with *hypoxanthine phosphoribosyltransferase 1 (HPRT1)*[52] for mRNAs and 18S rRNA for miRNAs as endogenous references.

Western blotting analysis. A protocol for this procedure was described previously.[53] For acetylated histone 3 and histone 4, equal protein was loaded and confirmed by ponceau S staining. For MyoD, blots were probed with glyceraldehyde 3-phosphate dehydrogenase (GAPDH) antibody to correct for differences in protein loading. Western blotting was performed with the following primary antibodies: MyoD (1:1000, sc-31940 X, Santa Cruz), acetyl-histone H3 (0.05 μg/ml, 06-599, Millipore), acetyl-histone H4 (1:1000, 06-866, Millipore), GAPDH (1:3000, sc-20357, Abcam), followed by horseradish peroxidase (HRP)-conjugated secondary antibodies (donkey anti-goat, 1:3000, sc-2020, Santa Cruz; goat anti-rabbit, 1:2000, sc-2004, Santa

©2012 Landes Bioscience. Do not distribute.

Cruz). Finally, the specific signals were detected by chemiluminescence using the SuperSignal West Pico Chemiluminescent Substrate (34077, Thermo Scientific). Images were acquired by Quantity One 1-D analysis software (Bio-Rad).

DNA methylation study. The 5'-regulatory region of *FST* (GenBank: M19529) was submitted to the online program Methprimer[54] to identify the CpG islands. Genomic DNA (1 μg) was subjected to bisulfite modification using EZ DNA Methylation-Direct Kit (D5020, Zymo Research) according to the manufacturer's protocol. The *FST* 5'-regulatory region containing CpG island was amplified by nested PCR with FST-met-nest primer pairs (**Table 1**) designed using PerlPrimer[55] and Methyl Primer Express Software v1.0 (Applied Biosystems Inc.). PCR products were purified with QIAquick PCR purification kit (28104, Qiagen) and then subcloned into the pGEM T-easy vector (A1360, Promega). A minimum of six different positive clones were randomly selected for sequencing with M13 primers performed by the CEQ8000 sequencer system (Beckman Coulter). The final sequence results were processed by QUMA software.[56] Sequences with a conversion rate below 90% were excluded from analysis.

ChIP assays. The chromatin immunoprecipitation (ChIP) assay kit (17-295, Millipore) was used in accordance with the manufacturer's instructions. Soluble chromatin was immunoprecipitated with anti-MyoD (sc-31940 X, Santa Cruz), anti-acetyl-histone H3 (06-599, Millipore) or anti-acetyl-histone H4 (06-866, Millipore). Immunoprecipitates were subjected to quantitative PCR with *MSTN* promoter specific primers spanning the putative binding sites of interest (**Table 1**). As a negative control, a primer pair of MyoD binding site free region was used to amplify another genomic region that was not expected to interact with MyoD. Antibodies against RNA polymerase II (sc-899 X, Santa Cruz) and normal rabbit IgG (2729S, Cell signaling Technology) were used as a positive and a negative control in the assay, respectively. PCR products were separated on a 2% agarose gel stained with ethidium bromide for visualization. With the percent input method, signals obtained from the ChIP are divided by signals obtained from an input sample. Quantitative PCR data were normalized to and expressed as % of input.

Statistical analysis. Pairwise comparisons were made between treatment groups and the vehicle-treated control, using Student's t-test. The data were expressed as means ± standard deviations (SD) and $*p < 0.05$, $**p < 0.01$ and $***p < 0.001$ were set statistically significant.

Disclosure of Potential Conflicts of Interest

No potential conflicts of interest were disclosed.

Acknowledgments

This work was supported by the German Research Foundation (DFG) project Drip, grant nr. 753. Authors are grateful to Prof Dr Stephan Baader and Prof Dr Brigitte Schmitz at University Bonn for the utilization of laboratory facilities. Authors are also indebted to Ms Nadine Leyer for technical assistance and Mr. Ludger Buschen at the research station "Frankenforst" of Bonn University for organizing sample collection during the experiments.

References

1. Lunney JK. Advances in swine biomedical model genomics. Int J Biol Sci 2007; 3:179-84; PMID:17384736; http://dx.doi.org/10.7150/ijbs.3.179.
2. Wagers AJ, Conboy IM. Cellular and molecular signatures of muscle regeneration: current concepts and controversies in adult myogenesis. Cell 2005; 122:659-67; PMID:16143100; http://dx.doi.org/10.1016/j.cell.2005.08.021.
3. Kuang S, Gillespie MA, Rudnicki MA. Niche regulation of muscle satellite cell self-renewal and differentiation. Cell Stem Cell 2008; 2:22-31; PMID:18371418; http://dx.doi.org/10.1016/j.stem.2007.12.012.
4. Guerrero-Beltrán CE, Calderón-Oliver M, Pedraza-Chaverri J, Chirino YI. Protective effect of sulforaphane against oxidative stress: recent advances. Exp Toxicol Pathol 2012; 64:503-8; PMID:21129940; http://dx.doi.org/10.1016/j.etp.2010.11.005.
5. Myzak MC, Karplus PA, Chung FL, Dashwood RH. A novel mechanism of chemoprotection by sulforaphane: inhibition of histone deacetylase. Cancer Res 2004; 64:5767-74; PMID:15313918; http://dx.doi.org/10.1158/0008-5472.CAN-04-1326.
6. Myzak MC, Hardin K, Wang R, Dashwood RH, Ho E. Sulforaphane inhibits histone deacetylase activity in BPH-1, LnCaP and PC-3 prostate epithelial cells. Carcinogenesis 2006; 27:811-9; PMID:16280330; http://dx.doi.org/10.1093/carcin/bgi265.
7. Myzak MC, Dashwood WM, Orner GA, Ho E, Dashwood RH. Sulforaphane inhibits histone deacetylase in vivo and suppresses tumorigenesis in Apc-minus mice. FASEB J 2006; 20:506-8; PMID:16407454.
8. Myzak MC, Tong P, Dashwood WM, Dashwood RH, Ho E. Sulforaphane retards the growth of human PC-3 xenografts and inhibits HDAC activity in human subjects. Exp Biol Med (Maywood) 2007; 232:227-34; PMID:17259330.
9. McPherron AC, Lee SJ. Double muscling in cattle due to mutations in the myostatin gene. Proc Natl Acad Sci U S A 1997; 94:12457-61; PMID:9356471; http://dx.doi.org/10.1073/pnas.94.23.12457.
10. McCroskery S, Thomas M, Maxwell L, Sharma M, Kambadur R. Myostatin negatively regulates satellite cell activation and self-renewal. J Cell Biol 2003; 162:1135-47; PMID:12963705; http://dx.doi.org/10.1083/jcb.200207056.
11. Joulia-Ekaza D, Cabello G. The myostatin gene: physiology and pharmacological relevance. Curr Opin Pharmacol 2007; 7:310-5; PMID:17374508; http://dx.doi.org/10.1016/j.coph.2006.11.011.
12. Perdiguero E, Sousa-Victor P, Ballestar E, Muñoz-Cánoves P. Epigenetic regulation of myogenesis. Epigenetics 2009; 4:541-50; PMID:20009536; http://dx.doi.org/10.4161/epi.4.8.10258.
13. Kelly TK, De Carvalho DD, Jones PA. Epigenetic modifications as therapeutic targets. Nat Biotechnol 2010; 28:1069-78; PMID:20944599; http://dx.doi.org/10.1038/nbt.1678.
14. Drummond MJ, Glynn EL, Fry CS, Dhanani S, Volpi E, Rasmussen BB. Essential amino acids increase microRNA-499, -208b, and -23a and downregulate myostatin and myocyte enhancer factor 2C mRNA expression in human skeletal muscle. J Nutr 2009; 139:2279-84; PMID:19828686; http://dx.doi.org/10.3945/jn.109.112797.
15. Allen DL, Loh AS. Posttranscriptional mechanisms involving microRNA-27a and b contribute to fast-specific and glucocorticoid-mediated myostatin expression in skeletal muscle. Am J Physiol Cell Physiol 2011; 300:C124-37; PMID:20980549; http://dx.doi.org/10.1152/ajpcell.00142.2010.
16. Allen DL, Unterman TG. Regulation of myostatin expression and myoblast differentiation by FoxO and SMAD transcription factors. Am J Physiol Cell Physiol 2007; 292:C188-99; PMID:16885393; http://dx.doi.org/10.1152/ajpcell.00542.2005.
17. Ma K, Mallidis C, Artaza J, Taylor W, Gonzalez-Cadavid N, Bhasin S. Characterization of 5'-regulatory region of human myostatin gene: regulation by dexamethasone in vitro. Am J Physiol Endocrinol Metab 2001; 281:E1128-36; PMID:11701425.
18. Krauss RS. Evolutionary conservation in myoblast fusion. Nat Genet 2007; 39:704-5; PMID:17534361; http://dx.doi.org/10.1038/ng0607-704.
19. Singh SV, Srivastava SK, Choi S, Lew KL, Antosiewicz J, Xiao D, et al. Sulforaphane-induced cell death in human prostate cancer cells is initiated by reactive oxygen species. J Biol Chem 2005; 280:19911-24; PMID:15764812; http://dx.doi.org/10.1074/jbc.M412443200.
20. Pledgie-Tracy A, Sobolewski MD, Davidson NE. Sulforaphane induces cell type-specific apoptosis in human breast cancer cell lines. Mol Cancer Ther 2007; 6:1013-21; PMID:17339367; http://dx.doi.org/10.1158/1535-7163.MCT-06-0494.
21. Utriainen P, Liu J, Kuulasmaa T, Voutilainen R. Inhibition of DNA methylation increases follistatin expression and secretion in the human adrenocortical cell line NCI-H295R. J Endocrinol 2006; 188:305-10; PMID:16461556; http://dx.doi.org/10.1677/joe.1.06392.

©2012 Landes Bioscience. Do not distribute.

22. Iezzi S, Cossu G, Nervi C, Sartorelli V, Puri PL. Stage-specific modulation of skeletal myogenesis by inhibitors of nuclear deacetylases. Proc Natl Acad Sci U S A 2002; 99:7757-62; PMID:12032356; http://dx.doi.org/10.1073/pnas.112218599.
23. Iezzi S, Di Padova M, Serra C, Caretti G, Simone C, Maklan E, et al. Deacetylase inhibitors increase muscle cell size by promoting myoblast recruitment and fusion through induction of follistatin. Dev Cell 2004; 6:673-84; PMID:15130492; http://dx.doi.org/10.1016/S1534-5807(04)00107-8.
24. Gomyo Y, Sasaki J, Branch C, Roth JA, Mukhopadhyay T. 5-aza-2'-deoxycytidine upregulates caspase-9 expression cooperating with p53-induced apoptosis in human lung cancer cells. Oncogene 2004; 23:6779-87; PMID:15273730; http://dx.doi.org/10.1038/sj.onc.1207381.
25. Singh AV, Xiao D, Lew KL, Dhir R, Singh SV. Sulforaphane induces caspase-mediated apoptosis in cultured PC-3 human prostate cancer cells and retards growth of PC-3 xenografts in vivo. Carcinogenesis 2004; 25:83-90; PMID:14514658; http://dx.doi.org/10.1093/carcin/bgg178.
26. Lee SJ. Regulation of muscle mass by myostatin. Annu Rev Cell Dev Biol 2004; 20:61-86; PMID:15473835; http://dx.doi.org/10.1146/annurev.cellbio.20.012103.135836.
27. Amthor H, Nicholas G, McKinnell I, Kemp CF, Sharma M, Kambadur R, et al. Follistatin complexes Myostatin and antagonises Myostatin-mediated inhibition of myogenesis. Dev Biol 2004; 270:19-30; PMID:15136138; http://dx.doi.org/10.1016/j.ydbio.2004.01.046.
28. Valencia-Sanchez MA, Liu J, Hannon GJ, Parker R. Control of translation and mRNA degradation by miRNAs and siRNAs. Genes Dev 2006; 20:515-24; PMID:16510870; http://dx.doi.org/10.1101/gad.1399806.
29. Callis TE, Pandya K, Seok HY, Tang RH, Tatsuguchi M, Huang ZP, et al. MicroRNA-208a is a regulator of cardiac hypertrophy and conduction in mice. J Clin Invest 2009; 119:2772-86; PMID:19726871; http://dx.doi.org/10.1172/JCI36154.
30. Bell ML, Buvoli M, Leinwand LA. Uncoupling of expression of an intronic microRNA and its myosin host gene by exon skipping. Mol Cell Biol 2010; 30:1937-45; PMID:20154144; http://dx.doi.org/10.1128/MCB.01370-09.
31. Bendixen E, Danielsen M, Larsen K, Bendixen C. Advances in porcine genomics and proteomics--a toolbox for developing the pig as a model organism for molecular biomedical research. Brief Funct Genomics 2010; 9:208-19; PMID:20495211; http://dx.doi.org/10.1093/bfgp/elq004.
32. Malaguti M, Angeloni C, Garatachea N, Baldini M, Leoncini E, Collado PS, et al. Sulforaphane treatment protects skeletal muscle against damage induced by exhaustive exercise in rats. J Appl Physiol 2009; 107:1028-36; PMID:19713431; http://dx.doi.org/10.1152/japplphysiol.00293.2009.
33. Zhou H, Brockington M, Jungbluth H, Monk D, Stanier P, Sewry CA, et al. Epigenetic allele silencing unveils recessive RYR1 mutations in core myopathies. Am J Hum Genet 2006; 79:859-68; PMID:17033962; http://dx.doi.org/10.1086/508500.
34. Meeran SM, Patel SN, Tollefsbol TO. Sulforaphane causes epigenetic repression of hTERT expression in human breast cancer cell lines. PLoS One 2010; 5:e11457; PMID:20625516; http://dx.doi.org/10.1371/journal.pone.0011457.
35. Hsu A, Wong CP, Yu Z, Williams DE, Dashwood RH, Ho E. Promoter de-methylation of cyclin D2 by sulforaphane in prostate cancer cells. Clin Epigenetics 2011; 3:3; PMID:22303414; http://dx.doi.org/10.1186/1868-7083-3-3.
36. Ping Z, Liu W, Kang Z, Cai J, Wang Q, Cheng N, et al. Sulforaphane protects brains against hypoxic-ischemic injury through induction of Nrf2-dependent phase 2 enzyme. Brain Res 2010; 1343:178-85; PMID:20417626; http://dx.doi.org/10.1016/j.brainres.2010.04.036.
37. Dashwood RH, Ho E. Dietary histone deacetylase inhibitors: from cells to mice to man. Semin Cancer Biol 2007; 17:363-9; PMID:17555985; http://dx.doi.org/10.1016/j.semcancer.2007.04.001.
38. Park JH, Jung Y, Kim TY, Kim SG, Jong HS, Lee JW, et al. Class I histone deacetylase-selective novel synthetic inhibitors potently inhibit human tumor proliferation. Clin Cancer Res 2004; 10:5271-81; PMID:15297431; http://dx.doi.org/10.1158/1078-0432.CCR-03-0709.
39. Lee SJ, Lee YS, Zimmers TA, Soleimani A, Matzuk MM, Tsuchida K, et al. Regulation of muscle mass by follistatin and activins. Mol Endocrinol 2010; 24:1998-2008; PMID:20810712; http://dx.doi.org/10.1210/me.2010-0127.
40. Han DS, Huang HP, Wang TG, Hung MY, Ke JY, Chang KT, et al. Transcription activation of myostatin by trichostatin A in differentiated C2C12 myocytes via ASK1-MKK3/4/6-JNK and p38 mitogen-activated protein kinase pathways. J Cell Biochem 2010; 111:564-73; PMID:20568119; http://dx.doi.org/10.1002/jcb.22740.
41. Cho JS, Moon YM, Park IH, Um JY, Moon JH, Park SJ, et al. Epigenetic regulation of myofibroblast differentiation and extracellular matrix production in nasal polyp-derived fibroblasts. Clin Exp Allergy 2012; 42:872-82; http://dx.doi.org/10.1111/j.1365-2222.2011.03931.x; PMID:22239687.
42. Liu X, Wang J, Li R, Yang X, Sun Q, Albrecht E, et al. Maternal dietary protein affects transcriptional regulation of myostatin gene distinctively at weaning and finishing stages in skeletal muscle of Meishan pigs. Epigenetics 2011; 6:899-907; PMID:21597337; http://dx.doi.org/10.4161/epi.6.7.16005.
43. Saito Y, Liang G, Egger G, Friedman JM, Chuang JC, Coetzee GA, et al. Specific activation of microRNA-127 with downregulation of the proto-oncogene BCL6 by chromatin-modifying drugs in human cancer cells. Cancer Cell 2006; 9:435-43; PMID:16766263; http://dx.doi.org/10.1016/j.ccr.2006.04.020.
44. Wiklund ED, Bramsen JB, Hulf T, Dyrskjøt L, Ramanathan R, Hansen TB, et al. Coordinated epigenetic repression of the miR-200 family and miR-205 in invasive bladder cancer. Int J Cancer 2011; 128:1327-34; PMID:20473948; http://dx.doi.org/10.1002/ijc.25461.
45. Scott GK, Mattie MD, Berger CE, Benz SC, Benz CC. Rapid alteration of microRNA levels by histone deacetylase inhibition. Cancer Res 2006; 66:1277-81; PMID:16452179; http://dx.doi.org/10.1158/0008-5472.CAN-05-3632.
46. Spiller MP, Kambadur R, Jeanplong F, Thomas M, Martyn JK, Bass JJ, et al. The myostatin gene is a downstream target gene of basic helix-loop-helix transcription factor MyoD. Mol Cell Biol 2002; 22:7066-82; PMID:12242286; http://dx.doi.org/10.1128/MCB.22.20.7066-7082.2002.
47. ZDS. Zentralverband der Deutschen Schweineproduktion (ZDS): Richtlinie für die Stationsprüfung auf Mastleistung, Schlachtkörperwert und Fleischbeschaffenheit beim Schwein. 2003.
48. Mau M, Oksbjerg N, Rehfeldt C. Establishment and conditions for growth and differentiation of a myoblast cell line derived from the semimembranosus muscle of newborn piglets. In Vitro Cell Dev Biol Anim 2008; 44:1-5; PMID:18074188; http://dx.doi.org/10.1007/s11626-007-9069-6.
49. Lewis BP, Shih IH, Jones-Rhoades MW, Bartel DP, Burge CB. Prediction of mammalian microRNA targets. Cell 2003; 115:787-98; PMID:14697198; http://dx.doi.org/10.1016/S0092-8674(03)01018-3.
50. Rozen S, Skaletsky H. Primer3 on the WWW for general users and for biologist programmers. Methods Mol Biol 2000; 132:365-86; PMID:10547847.
51. Livak KJ, Schmittgen TD. Analysis of relative gene expression data using real-time quantitative PCR and the 2(-Delta Delta C(T)) Method. Methods 2001; 25:402-8; PMID:11846609; http://dx.doi.org/10.1006/meth.2001.1262.
52. Uddin MJ, Cinar MU, Tesfaye D, Looft C, Tholen E, Schellander K. Age-related changes in relative expression stability of commonly used housekeeping genes in selected porcine tissues. BMC Res Notes 2011; 4:441; PMID:22023805; http://dx.doi.org/10.1186/1756-0500-4-441.
53. Fan H, Cinar MU, Phatsara C, Tesfaye D, Tholen E, Looft C, et al. Molecular mechanism underlying the differential MYF6 expression in postnatal skeletal muscle of Duroc and Pietrain breeds. Gene 2011; 486:8-14; PMID:21749918; http://dx.doi.org/10.1016/j.gene.2011.06.031.
54. Li LC, Dahiya R. MethPrimer: designing primers for methylation PCRs. Bioinformatics 2002; 18:1427-31; PMID:12424112; http://dx.doi.org/10.1093/bioinformatics/18.11.1427.
55. Marshall OJ. PerlPrimer: cross-platform, graphical primer design for standard, bisulphite and real-time PCR. Bioinformatics 2004; 20:2471-2; PMID:15073005; http://dx.doi.org/10.1093/bioinformatics/bth254.
56. Kumaki Y, Oda M, Okano M. QUMA: quantification tool for methylation analysis. Nucleic Acids Res 2008; 36(Web Server issue):W170-5; PMID:18487274; http://dx.doi.org/10.1093/nar/gkn294.

©2012 Landes Bioscience. Do not distribute.